

## CHAPTER 7

# *Quantum Effects in Enzyme Kinetics*

ARUNDHUTI SEN AND AMNON KOHEN

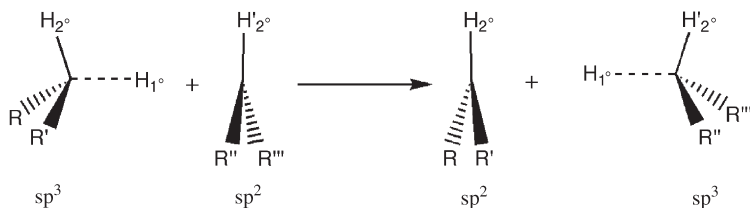
Department of Chemistry, University of Iowa, Iowa City, IA 52242, USA

### 7.1 Introduction

Historically, the study of enzymatic catalysis has been characterised by multidisciplinary approaches to the investigation of a range of issues: structural features relevant to catalysis, substrate binding and product-release patterns, the role of functional residues (*e.g.* general bases or acids) *etc.* One contemporary topic in enzymology is that of quantum-mechanical effects, including zero-point energies (ZPE) and quantum tunnelling, and the contribution these physical phenomena make to enzyme catalysis.<sup>1</sup> As mentioned in previous chapters, traditional theories of enzymatic catalysis focus on concepts such as transition-state stabilisation and ground-state destabilisation to account for the enormous rate enhancements seen in enzyme reactions.<sup>1,2</sup> These concepts were grounded in classical transition-state theory, which did not consider quantum-mechanical effects. In the past two decades, however, experimental data demonstrating tunnelling and related quantum effects in enzymes has given rise to a number of theoretical models that attempt to rationalise the empirical findings. Some of these models (the Bell correction to transition-state theory, various ‘Marcus-like’ models) have been elaborated

---

<sup>1</sup>It should be noted that any attempt to separate catalysis into constituent additive contributions is a somewhat artificial process, since the quantitative degree of each contribution is inherently model dependent.



AQI

**Figure 7.1** The general H-transfer reaction used as a model reaction in the text.

upon in the previous chapters, and their individual importance can be gauged by their ability to interpret and explain experimental findings. The present chapter focuses on a significant experimental tool used to examine tunnelling and coupled motion in enzymatic systems, *viz.* kinetic isotope effects (KIEs).

The kinetic isotope effect is simply the ratio of rates between two molecules that differ only in their isotopic composition (isotopologues), and has traditionally been one of the most useful probes of the potential-energy surface for organic reactions. A well-designed KIE<sup>ii</sup> experiment can, in essence, focus on the chemical step of an enzyme reaction within the intricate kinetic pathway associated with enzymatic catalysis, thus providing information only about the mechanistic step of interest. For example, when the reaction under consideration is a H-transfer reaction, as in Figure 7.1, then the KIEs for protium, deuterium, and tritium-labelled substrates may provide substantial information about the reaction coordinate and the nature of the transition state.<sup>3</sup> H-transfer reactions are particularly interesting since (i) due to the large mass ratio of D/H (2) and T/H (3) the KIEs are large, and (ii) due to the small mass of hydrogen, quantum effects are more likely to be significant. The de Broglie wavelength of the hydrogen atom corresponds to the H-transfer distance in many biological systems, which in turn corresponds to the width of the barrier that must be traversed for tunnelling to occur.<sup>4</sup> Enzymatic reactions that involve H-transfer are thus excellent cases with which to investigate the role of quantum-mechanical tunnelling in catalysis.

The following section (7.2) provides an introduction to the terminology and theory of kinetic isotope effects, as well as a discussion of two important mathematical formulations: the Swain–Schaad relationships for 1° and 2° KIEs, and the Northrop equations for the extraction of intrinsic KIEs from observed values. Section 7.3 describes the ways in which KIEs can be used to probe tunnelling and coupled motion in enzymatic systems, and Section 7.4 summarises recent examples from studies of three different systems: alcohol dehydrogenase, dihydrofolate reductase and thymidylate synthase.

<sup>ii</sup> A ‘well-designed’ KIE experiment would ensure that only the kinetic step of interest is isotopically sensitive, and that the intrinsic KIE on this step is not masked by other kinetic steps.

## 7.2 Kinetic Isotope Effects: Basic Terms and Concepts

### 7.2.1 Defining KIEs

The Bigeleisen equation defines the kinetic isotope effect for two isotopically labelled systems in terms of their partition functions. Thus, for reactants labelled with light ( $L$ ) and heavy ( $H$ ) isotopes, with reaction rates  $k_L$  and  $k_H$ , respectively, the KIE would be expressed as follows:

$$\text{KIE} = \frac{k_L}{k_H} = (\kappa_L/\kappa_H)^* \text{ZPE}^* \text{MMI}^* \text{EXC} \quad (7.1)$$

where  $\kappa$  is the transmission coefficient and the other terms are the isotope effects on the zero-point energies (ZPE), on the rotational and translational energies (mass moments of inertia or MMI), and on populations of excited vibrational states (EXC)<sup>5,6</sup>. Since the rate of a reaction is exponentially related to the activation barrier for that reaction, the ratio of rates (KIE) is proportional to the difference in activation free energies of the light and heavy isotopes:

$$\text{KIE} = \frac{k_L}{k_H} \approx e^{(\Delta G_H^\ddagger - \Delta G_L^\ddagger)/RT} \quad (7.2)$$

In most cases, the difference in activation energy between isotopologues, *i.e.*  $\Delta G_H^\ddagger - \Delta G_L^\ddagger$ , can largely be attributed to the change in zero-point energies between the ground state and transition state for each reactant (Figure 7.2).<sup>7</sup>

The very definition of the KIE allows for considerable variation in experimental design, particularly in the following respects: (i) the manner in which the KIE is measured and (ii) the selection of labelling patterns for the isotopologue reactants. Based on the position of the labelled atom relative to the atom being transferred, two kinds of KIE can be defined: primary ( $1^\circ$ ) KIEs, measured for a bond cleavage or formation wherein one of the bound atoms is isotopically labelled, and secondary ( $2^\circ$ ) KIEs, where the labelled atom is not one of the atoms participating in bond cleavage or formation.  $2^\circ$  KIEs result from changes in bonding force constants and vibrational frequencies during the reaction, and generally have smaller values than  $1^\circ$  KIEs. Additionally, KIE values can be broadly classified as normal or inverse, where normal values are those above 1 (*i.e.* the lighter isotope transferred faster than the heavier one) and inverse KIEs are smaller than 1 (the heavier isotope transferred faster than the lighter one). Another term relevant to the discussion of KIEs is the equilibrium isotope effect (EIE). Unlike KIEs, EIEs are not dependent on transition-state properties, but arise from the equilibrium distribution of isotopes between two stable states, such as the reactant and the product states in a given reaction. In other words, the EIE is affected by changes when going from reactants to products, while the KIE originates in differences between the ground state and the transition state.

At the simplest level, the value of the KIE can be used to assess the location of the transition state (late or early) and the nature of the change in bond order

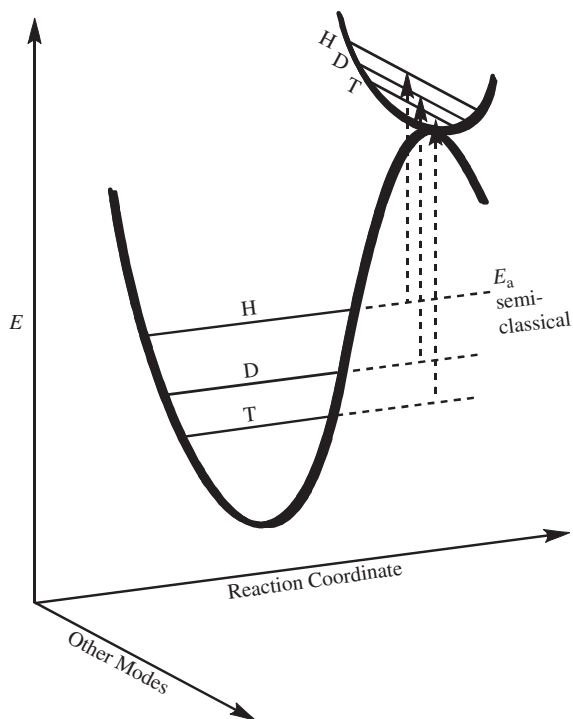


**Figure 7.2** Different energies of activation ( $\Delta E_a$ ) for H, D, and T, resulting from their different zero-point energies (ZPE) at the ground state (GS) and transition state (TS). The GS-ZPE is constituted by all degrees of freedom but mostly by the C-H stretching frequency, and the TS-ZPE is constituted by all degrees of freedom orthogonal to the reaction coordinate. This type of consideration is depicted as “semiclassical”.

( $sp^3$  to  $sp^2$ , etc.). For example, the magnitude of  $2^\circ$  KIEs have traditionally been compared to the reaction's  $2^\circ$  EIE in order to determine whether the reaction had an early or late transition state.<sup>3</sup> This simple analysis assumes that the bond order of the  $2^\circ$  labelled atom is changing in proportion to the reaction progress and that the maximum change is reached at the product state. According to this model, the  $2^\circ$  EIE will be the larger value and will express the full magnitude of the change, while the  $2^\circ$  KIE will be between unity (for an early transition state) and the EIE (for a late transition state). More recently, it has been suggested that simple comparisons between  $2^\circ$  EIE and KIE values are not good indicators of the position of the transition state, due to the number and complexity of factors influencing the  $2^\circ$  KIE.<sup>8-12</sup>

### 7.2.2 Swain–Schaad Relationships for $1^\circ$ and $2^\circ$ KIEs

Equation (7.1) is considered semiclassical since certain quantum-mechanical effects (such as ZPE) are included in the description and others, such as

tunnelling, are left out. Within this semiclassical description, the kinetic relationship among the three isotopes of hydrogen is determined, for the most part, by their relative ZPEs at the ground *vs.* transition states (Figure 7.2). The relationship among the three reaction rates can be developed quite simply from the reduced masses of the isotopes involved, to give the Swain–Schaad exponential relationship first defined by Swain *et al.* in 1958:<sup>13</sup>

$$\frac{k_{\text{H}}}{k_{\text{T}}} = \left(\frac{k_{\text{H}}}{k_{\text{D}}}\right)^{\text{EXP}} \quad \text{or} \quad \text{SSE} = \frac{\ln(k_{\text{H}}/k_{\text{T}})}{\ln(k_{\text{H}}/k_{\text{D}})} \quad (7.3)$$

where  $k_i$  is the reaction rate constant for isotope  $i$ , and SSE denotes the Swain–Schaad exponent. SSE is calculated from eqn (7.1) as follows:

$$\text{SSE} = \frac{\ln(k_{\text{H}}/k_{\text{T}})}{\ln(k_{\text{H}}/k_{\text{D}})} = \frac{1/\sqrt{\mu_{\text{H}}} - 1/\sqrt{\mu_{\text{T}}}}{1/\sqrt{\mu_{\text{H}}} - 1/\sqrt{\mu_{\text{D}}}} \quad (7.4)$$

where  $\mu_i$  is the reduced mass of the isotope  $i$ . The exponent thus calculated for H/T *vs.* H/D KIEs has a value of 1.42 (a value of 1.44 is calculated using atomic masses). When the experiment calls for labelling patterns that use T as the reference isotope, to obtain H/T *vs.* D/T KIEs, the equation for SSE is modified accordingly:

$$\text{SSE} = \frac{\ln(k_{\text{H}}/k_{\text{T}})}{\ln(k_{\text{D}}/k_{\text{T}})} = \frac{1/\sqrt{\mu_{\text{H}}} - 1/\sqrt{\mu_{\text{T}}}}{1/\sqrt{\mu_{\text{D}}} - 1/\sqrt{\mu_{\text{T}}}} \quad (7.5)$$

The SSE calculated from eqn (7.4) has a value of 3.26 (for atomic masses, and 3.34 using reduced masses). The utility of the Swain–Schaad relationships lies in their simplicity, and apparent independence from many of the factors influencing the reaction potential surface. Due to this latter quality, the Swain–Schaad equations can be used to relate unknown intrinsic KIEs to observed values, as in the Northrop method (Section 7.2.3). Other applications include the use of the 2° Swain–Schaad exponents (2° SSEs) as a probe for tunnelling and as an indicator of coupled motion between primary and secondary hydrogens for hydride-transfer reactions (Section 7.3.2).

### 7.2.3 Kinetic Complexity

As mentioned previously, KIEs provide direct insights into the nature of H-transfer reactions and the associated potential-energy surfaces. However, one limitation of the KIE technique should be evident upon inspection of eqn (7.1): in order to use the KIE as a probe of the H-transfer step, the H-transfer step must indeed be the ‘rate limiting’ (slowest) step of the enzymatic reaction. Most enzyme reactions consist of a complex series of events (such as binding of substrate, conformational changes of reactive intermediates, product release,

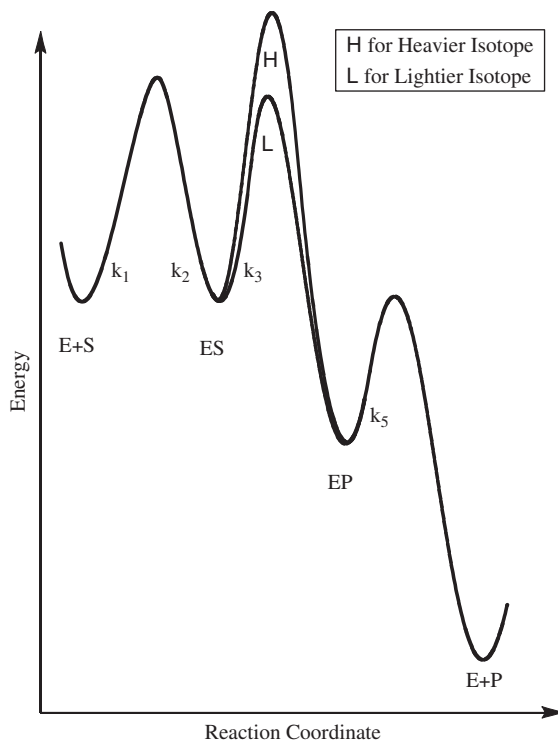
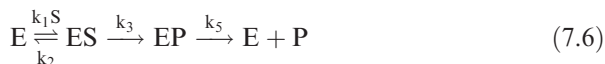


**Figure 7.3** An illustration of a reaction coordinate for the mechanism shown in Eq. 7.6.

*etc.*), each of which can be rate-limiting under the appropriate conditions. In such cases, KIE measurements must be conducted with due consideration of the following questions:

1. Is the KIE measured truly an ‘intrinsic’ KIE (*i.e.* measured on a single kinetic step) or is it being measured on a kinetically complex rate constant (*e.g.*  $k_{\text{cat}}/K_M$  or  $k_{\text{cat}}$ )?
2. Are steps other than the one under consideration isotopically sensitive?

These points can be illustrated using a relatively simple, single substrate reaction mechanism as follows (Figure 7.3):



If the KIE on the chemical step is to be measured, the rate constant  $k_3$  alone must be isotopically sensitive, since the conversion from ES to EP involves the bond-breaking and formation steps. However, unless the bond-breaking step is the slowest step in the reaction ( $k_3 \ll k_1, k_2, k_5$ ), the observed isotope effect on  $k_3$

will be masked by the rates of the preceding and following isotopically insensitive steps. This phenomenon is called kinetic complexity. For 1° KIEs, such kinetic complexity and the resultant experimental artifacts cause the observed KIE ( $KIE_{\text{obs}}$ ) to be smaller than the intrinsic KIE ( $KIE_{\text{int}}$ ).

Mathematically, kinetic complexity can be expressed in terms of the commitment to catalysis, or the ratio between the isotopically sensitive steps and the isotopically nonsensitive steps that lead to the decomposition of the reactive complex. The relationship between  $KIE_{\text{obs}}$ ,  $KIE_{\text{int}}$  and the forward and reverse commitments to catalysis ( $C_f$  and  $C_r$ , respectively) is given by the expression:<sup>14,15</sup>

$$KIE_{\text{obs}} = \frac{KIE_{\text{int}} + C_f + C_r \cdot EIE}{1 + C_f + C_r} \quad (7.7)$$

Here,  $C_f$  is the ratio between the rate of the isotopically sensitive step forward and the rates of the preceding isotopically insensitive steps backward;  $C_r$  is the ratio between the rates of the isotopically sensitive step backward and the succeeding isotopically insensitive steps forward. For the reaction given by eqn (7.6),  $C_f = k_3/k_2$  and  $C_r = k_3/k_5$ .<sup>16</sup>

With some algebraic modification, eqn (7.7) can be used in combination with the Swain–Schaad exponents to calculate the commitments to catalysis and, more importantly, to calculate the  $KIE_{\text{int}}$  from  $KIE_{\text{obs}}$ . This technique was developed by Dexter B. Northrop, and assumes close concurrence between the intrinsic 1° SSEs and their semiclassically predicted values. The details of this method have been described elsewhere<sup>17,18</sup> and are not presented in this chapter; the final result allows calculation of an intrinsic KIE (*e.g.*,  $(k_H/k_T)_{\text{int}}$  in eqn (7.8) when two observed KIE values are available ( $(k_H/k_D)_{\text{obs}}$  and  $(k_H/k_T)_{\text{obs}}$ ):

$$\frac{(k_H/k_T)_{\text{obs}} - 1}{(k_H/k_D)_{\text{obs}} - 1} = \frac{(k_H/k_T)_{\text{int}} - 1}{((k_H/k_T)_{\text{int}})^{1/1.44} - 1} \quad (7.8)$$

Equation (7.8) cannot be solved analytically (due to transcendental functions) and must be solved numerically once values are available for the observed KIEs.<sup>iii,iv</sup> Intrinsic KIEs are directly relevant to the reaction potential surface of a specific barrier, and can thus be compared to theoretical calculations that commonly focus on a single step. Practically, the Northrop method

<sup>iii</sup> References [17,18] include tables containing numerical solutions for a wider range of KIEs. Today, these can easily be calculated with a calculator or computer, see <http://cricket.chem.uiowa.edu/~kohen/tools.html>

<sup>iv</sup> In cases where the chemical step is reversible and a small 1° EIE cannot be assumed, a numerical solution requires the calculation of the reverse commitment ( $C_r$ ). For such cases, Cleland has identified a range for the  $KIE_{\text{int}}$  values between the observed KIE and the product of the EIE and  $KIE_{\text{obs}}$  for the reverse reaction ( $KIE_{\text{obs-rev}} \cdot EIE$ ).<sup>19</sup>

removes the kinetic complexity and unmasks the intrinsic KIE, which is the value of interest in mechanistic enzymology.

## 7.2.4 Coupling and Coupled Motion

In mechanistic enzymology, the term ‘coupling’ is applied to two distinct phenomena: (i) primary–secondary ( $1^\circ$ – $2^\circ$ ) coupled motion and (ii) environmentally coupled tunnelling. The first refers to H-transfer reactions and defines the coupling between the transferred hydrogen and another hydrogen bound to the donor or acceptor heavy atom. The second term refers to the way the tunnelling of the transferred hydrogen is coupled to the enzymatic environment, and is synonymous with other terms such as ‘tunnelling-promoting vibrations’ and ‘vibrationally enhanced tunnelling’. More generally, when two coordinates interact in such a way that a change in one coordinate affects the potential energy of the other, they are said to be coupled.<sup>v</sup> For example, when two hydrogens bound to the same carbon are coupled (as is the case for the alcohol dehydrogenase, Section 7.4.1), the cleavage of one C–H bond is not independent of the isotopic composition of the other hydrogen on the same carbon (or the acceptor carbon). In terms of bond vibrations, the stretching mode of one bond (that is converted into a translation at bond cleavage) is coupled to vibrational modes of the other.  $1^\circ$ – $2^\circ$  coupled motion is a phenomenon associated with tunnelling of the transferred atom, and in the case of H-transfer reactions can be exposed using mixed-labelling experiments (Section 7.2.5.2).

## 7.2.5 Experimental Methods and Design

### 7.2.5.1 Competitive vs. Noncompetitive KIE Measurements

KIE measurements can be performed in two distinct ways, *via* competitive or noncompetitive experiments. The noncompetitive method measures the rates of reaction for individual isotopologue reactants in separate experiments. Then, the rates are divided to yield the KIE and the errors from each measurement are propagated to the KIE. Competitive measurements involve a mixture of isotopologue substrates in a single reaction vessel. During the reaction, either the depletion of the heavy isotope in the product or its enrichment in the reactant is followed, and used to calculate the KIE directly (without needing to measure reaction rates). Each method has its own advantages and disadvantages: noncompetitive experiments, for example, measure the isotope effect on  $k_{\text{cat}}$  as well as  $k_{\text{cat}}/K_{\text{m}}$ , whereas competitive experiments can be shown to measure the isotope effect only on  $k_{\text{cat}}/K_{\text{m}}$ .<sup>14</sup> On the other hand, competitive measurements result in lower errors than the noncompetitive experiments, thus limiting the

<sup>v</sup>From the mathematical point of view, coupling may be defined as the mixing between two states (motion along two coordinates). Coupling matrix elements will be proportional to the second derivative of the potential energy with respect to both coordinates.

noncompetitive method to the measurement of KIEs greater than 1.25.<sup>20</sup> Additionally, noncompetitive KIEs cannot examine radioactive isotopes (e.g., T, due to the extreme levels of radioactivity needed while working with pure, 100% labelled, radioactive reactants), while in a competitive experiment the radioactive isotope is only present in a trace amount, enabling measurements of H/T and other KIEs. This makes competitive measurements more appealing, particularly when measuring small isotope effects involving radioactive materials such as 2° H/T, 1° D/T KIEs or heavy-atom KIEs.

### 7.2.5.2 Mixed-Labeling Experiments

An experimental method relevant to enzymatic tunnelling studies is mixed labelling of isotopologue reactants. These experiments are used when deviations in the 2° SSEs are sought as indicators of tunnelling (Section 7.3.3). Mixed-labelling experiments employ an isotopic labelling pattern than is more involved than that used in the original Swain–Schaad relationship, but are considered sensitive indicators of H-tunnelling.<sup>8,21,22</sup>

A mixed-labelling experiment would measure the 2° H/T KIE with H in the 1° position, and the 2° D/T KIE with D in the 1° position (Figure 7.4). These KIEs would be denoted by  $k_{HH}/k_{HT}$  and  $k_{DD}/k_{DT}$ , respectively, where  $k_{ij}$  is the rate constant for H-transfer with isotope  $i$  in the 1° position and isotope  $j$  in the 2° position. Thus, the 2° Swain–Schaad relationship can be expressed as:

$$2^{\circ}\text{MSE} = \frac{\ln(k_{HH}/k_{HT})}{\ln(k_{DD}/k_{DT})} \quad (7.9)$$

This mixed-labelling relationship is distinguished from the usual SSE by the exponent <sup>M</sup>SSE. The 2° <sup>M</sup>SSE is particularly interesting, since it is used as a probe for both tunnelling and coupled motion between 1° and 2° hydrogens (as explained in Section 7.3.3).

A rigorous mathematical treatment explaining the high sensitivity of the mixed-labelling experiment to H-tunnelling can be found in refs. 23 and 22. Huskey and Saunders both independently showed that very large values of <sup>M</sup>EXP are only calculated for 2° KIEs that arise from coupled motion and tunnelling in the system of interest.<sup>23–25</sup> Both concluded that the extra isotopic substitution at the geminal position is essential for the experimental design,

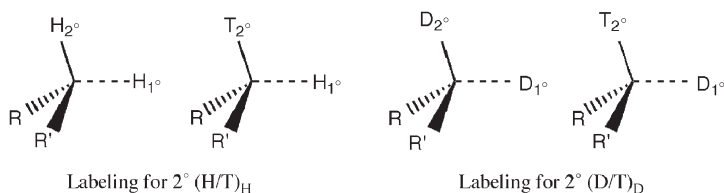


**Figure 7.4** The isotopic labeling pattern for a mixed-labeling experiment.

thus making a case for the mixed labelling method. More recent calculations have further emphasised the validity of this method, as well as limitations when applied in certain contexts.<sup>10,26</sup>

## 7.3 KIEs as Probes for Tunnelling

Once a set of intrinsic KIEs have been obtained (as described in Section 7.2), the results can be interpreted to clarify a variety of issues, such as transition-state geometry, mechanistic details, and quantum-mechanical effects. When studying tunnelling in enzymatic systems, the following three methods are frequently employed to obtain signatures of tunnelling: (i) comparing the magnitude of the KIE to that expected from eqn (7.1) (nontunnelling model); (ii) identifying cases of deviation of  $2^\circ \text{MSSSE}$  from the semiclassical expected values; and (iii) measuring the temperature dependence of the intrinsic KIEs and using both the difference in activation energies between the isotopes and the isotope effects on the Arrhenius pre-exponential factors to diagnose the extent of tunnelling in the system. The last method has the added advantage of being able to distinguish between data that comply with a tunnelling correction to the transition-state theory, and data that must be fitted to a Marcus-like model of tunnelling (see Chapter 5).

### 7.3.1 The Size of the KIE

For hydrogen-transfer reactions, the simplest indication of tunnelling is an anomalously large primary KIE that significantly exceeds the semiclassical limit (for H/D KIEs, this value is  $\sim 7$  at room temperature<sup>3</sup>). For instance, in the case of soybean lipoxygenase (SBL-1)<sup>27</sup> and galactose oxidase,<sup>28</sup> the sheer size of the  $1^\circ$  KIE was enough to suggest tunnelling. SBL-1 is an Fe(III)-dependent enzyme that catalyses the conversion of linoleic acid, an essential fatty acid, to 13(S)-hydroperoxy-9(Z), 11(E)-octadecanoic acid, with H-transfer being the rate-limiting step above 32 °C. The measured room-temperature H/D KIE for SBL-1 was  $\sim 81$ , and both proton and deuterium transfer rates as well as the KIEs themselves were weakly temperature dependent (see Section 7.4.3 for the temperature dependence of KIEs).<sup>27</sup> These two observations together (the large KIE value and temperature-dependent KIEs) can be interpreted as indicative of environmentally coupled tunnelling, especially since other explanations (magnetic coupling, branching of isotopically sensitive steps<sup>29</sup>) for the large KIE had already been discarded. Another system of interest in this context is galactose oxidase (GO), a radical-coupled copper oxidase catalysing the oxidation of a range of primary alcohols to produce aldehydes and hydrogen peroxide. At low substrate concentrations, substrate oxidation is the rate-determining step, and steady-state measurements under these conditions yielded large isotope effects (from 22.5 at 4 °C to 13 at 45 °C).<sup>28</sup> Once again, the large value of the KIE coupled with the strong temperature dependence of the KIEs was interpreted as indicative of tunnelling of the hydrogen atom at the rate-determining step.

### 7.3.2 Comparison of 2° KIEs and 2° EIEs

One of the first experimental indications of tunnelling in an enzymatic system came from kinetic studies of yeast formate dehydrogenase, an  $\text{NAD}^+$ -dependent enzyme that catalyses the conversion of formate to  $\text{CO}_2$ .<sup>30</sup> Blanchard and Cleland measured noncompetitive 2° H/D KIEs for  $\text{NAD}^+$ , using formate or deuterated formate as substrates (*i.e.* H or D in the 1° position). The measured intrinsic 2° H/D KIEs ( $1.23 \pm 0.03$  with H-transfer,  $1.07 \pm 0.02$  with D-transfer) were both larger than the measured EIE of 0.89.<sup>31</sup> From these results, they concluded that the reaction involved both coupling of the 1°–2° hydrogens as well as tunnelling from the 1° position. Tunnelling at the 1° position would explain the difference in the magnitude of the 2° KIE with replacement of the 1° H with D, as well as the larger size of the 2° KIE relative to the measured EIE.

### 7.3.3 Deviations from Semiclassical 2° Swain–Schaad Relationships

When it comes to tunnelling, eqn (7.5) is expected to be a much more sensitive probe than eqn (7.4). For 1° KIEs, the highest SSE values found in literature do not exceed 3.7; in fact, even in cases where other signs of tunnelling were evident (from mixed-labelling experiments or temperature-dependence studies of KIEs), the 1° SSE did not differ greatly from the semiclassical predicted values of 3.3 for  $\ln(k_{\text{H}}/k_{\text{T}})/\ln(k_{\text{D}}/k_{\text{T}})$  and 1.4 for  $\ln(k_{\text{H}}/k_{\text{T}})/\ln(k_{\text{H}}/k_{\text{D}})$ . Recent theoretical works have also provided support for the idea that tunnelling does not affect the value of the 1° SSE in a dramatic way.<sup>32,33</sup> Hence the semiclassical Swain–Schaad relationships can be used to calculate intrinsic KIEs from a set of observed KIEs. The method employed for this calculation is simply the Northrop method mentioned in Section 7.2.3.

The 2° <sup>M</sup>SSE, on the other hand, is more sensitive to tunnelling effects than its primary counterpart. When 2° KIEs are measured using mixed-labelling experiments (Section 7.2.5.2), an observed breakdown in the 2° Swain–Schaad relationship suggests both tunnelling and coupled motion between primary and secondary hydrogens. The expression for <sup>M</sup>SSE combines the rule of the geometric mean (RGM) and regular expression for the SSE. The RGM states that if the two hydrogens (1° and 2°) are independent of each other, the isotopic label at one position should not affect the isotope effect at the other.<sup>34</sup> Thus:

$$r = \frac{\ln(k_{\text{Hi}}/k_{\text{HT}})}{\ln(k_{\text{Di}}/k_{\text{DT}})} = 1 \quad (7.10)$$

with  $i = \text{H}$  or  $\text{D}$ . In the absence of coupling, the RGM predicts equivalence between the 2° SSE and the 2° <sup>M</sup>SSE:

$$2^\circ \text{SSE} = \frac{\ln(k_{\text{HH}}/k_{\text{HT}})}{\ln(k_{\text{HD}}/k_{\text{HT}})} = \frac{\ln(k_{\text{HH}}/k_{\text{HT}})}{\ln(k_{\text{DD}}/k_{\text{DT}})} = 2^\circ \text{M}^\circ \text{SSE} \quad (7.11)$$

However, if the motions of 1° and 2° hydrogens are coupled along the reaction coordinate, a breakdown of the RGM will result in an inflated 2°<sup>M</sup>SSE (*i.e.* 2°<sup>M</sup>SSE > 2° SSE).

The following rationalisation has often been used to explain why the 2°<sup>M</sup>SSE is a more sensitive indicator of coupled motion than the 1°<sup>M</sup>SSE: if the 1° and 2° hydrogens are coupled, the 1° KIE will have a secondary component, and will be deflated, but because the 2° H/D KIE is generally small, the deflation expected in the 1°<sup>M</sup>SSE is also very small. Conversely, the 2° KIE will have a primary component, which is much larger than the original 2° KIE. Thus, because H-tunnelling is more significant than D-tunnelling, coupling between 1° and 2° hydrogens results in an inflated 2°<sup>M</sup>SSE.

However, the KIEs for alcohol dehydrogenases (from various sources) and their relevant mutants reveal an interesting trend in the size of the 2°<sup>M</sup>SSE. From a survey of the available data, Klinman<sup>35</sup> reported relatively constant 2° H/T KIE values for a range of experiments, but a good correlation between the size of the 2° D/T KIE and that of the 2°<sup>M</sup>SSEs: as the magnitude of the 2° D/T KIE decreases, the 2°<sup>M</sup>SSE increases. This is an unexpected result considering the conventional rationalisation of deviations from the 2°<sup>M</sup>SSE. A proposed explanation for this sensitivity of 2° KIEs to D-transfer (rather than H-transfer) is based on steric hindrance at the active site. If the donor–acceptor distance in the active site has evolved for H-tunnelling, then D-transfer must require an abnormal decrease in this distance. However, a change in the donor–acceptor distance may cause a steric change in the environment surrounding the donor and acceptor atoms, which in turn could lead to a deflation of the 2° KIE.<sup>vi</sup>

### 7.3.4 Temperature Dependence of the KIEs

According to transition-state theory (TST), the reaction coordinate of an enzyme-catalysed reaction can be described in terms of a free-energy minimum and maximum, which correspond to the reactant well or ground state (GS) and the transition state (TS) respectively. Furthermore, GS and TS are assumed to be in pseudoequilibrium with each other, thus allowing their relative populations to be determined by the Boltzmann distribution. This simplifying assumption leads to the following exponential relationship between the reaction rate and the absolute temperature, generally known as the Arrhenius equation:

$$k = A \cdot e^{-(E_a/RT)} \quad (7.12)$$

where,  $A$  is the Arrhenius pre-exponential factor,  $E_a$  is the activation energy,  $T$  is the absolute temperature, and  $R$  is the gas constant. From eqn (7.12) and the

---

<sup>vi</sup>This intuitive explanation is yet to be addressed in a more rigorous fashion.

definition of the KIE, we obtain the following expression for the temperature dependence of KIEs:

$$\text{KIE} = \frac{k_L}{k_H} = \frac{A_L}{A_H} e^{\Delta E_{a(H-L)}/RT} \quad (7.13)$$

As long as the reaction is thermally activated, eqn (7.13) can be used to obtain values for  $A_L/A_H$  and  $\Delta E_{a(H-L)}$ . Since tunnelling from the GS is temperature independent, if tunnelling is the dominant contributor to the rates of both isotopes, the KIEs will be temperature independent. Thus,  $\Delta E_{a(H-L)}$  will be close to zero and  $A_L/A_H$  will be close to the KIEs at the experimental temperature. In the case of both thermal and tunnelling contributions, the extent of tunnelling can be assessed from the deviation of the Arrhenius parameters from these two extremes. At low temperatures, tunnelling contributions become significant enough that the Arrhenius plot begins to show nonlinear behaviour and we obtain curved plots (see Figure 7.5) whose significance has been discussed elsewhere.<sup>36</sup>

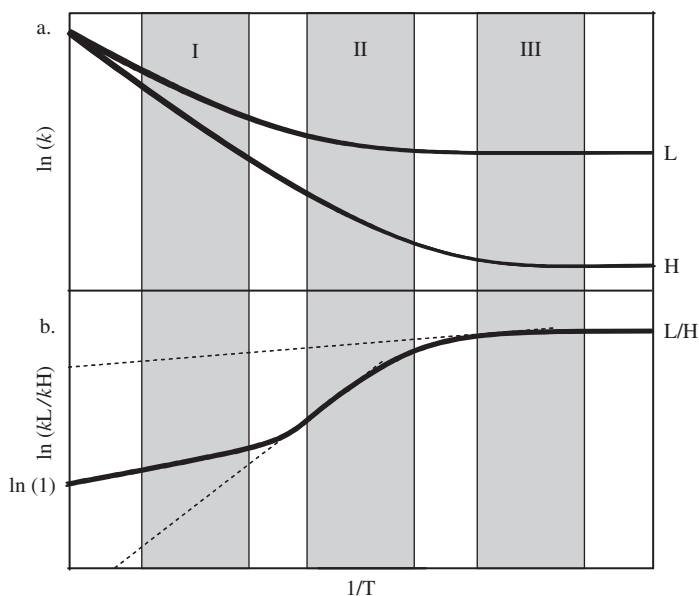


**Figure 7.5** An Arrhenius plot of a hydrogen transfer that is consistent with a tunneling correction to transition state theory. (a) Arrhenius plot of a light isotope (L) and heavy isotope (H). (b) Arrhenius plot of their KIE (L/H). Highlighted are experimental temperature ranges for three systems: I, a system with no tunneling contribution, II, a system with moderate tunneling, and III, a system with extensive tunneling contribution. The dashed lines are the tangents to the plot in each region.

The interpretation of KIE temperature dependence as a probe for tunnelling is a much discussed topic,<sup>4,37</sup> particularly in cases where the experimental data does not fit any of the aforementioned tunnelling regimes. This can occur when  $\Delta E_{a(H-L)}$  is close to zero but the  $\Delta H^\ddagger$  is not zero (in contrast to the prediction illustrated in region III in Figure 7.5). In these cases, it is common to favour Marcus-like models of tunnelling over tunnelling corrections to TST, as discussed in previous chapters in the current work (see Chapters 4 and 5).

## 7.4 Test Cases: Alcohol Dehydrogenase, Dihydrofolate Reductase and Thymidylate Synthase

The three enzymatic systems described below have all been studied using techniques that are described in Sections 7.2 and 7.3 (e.g. temperature dependence of KIEs, competitive mixed labelling measurements, *etc.*). While tunnelling behaviour has been observed in all three enzymes, alcohol dehydrogenase (ADH) has, to date, been the only system studied that has shown  $1^\circ$ – $2^\circ$  coupled motion (*via* a breakdown of the  $2^\circ$  Swain–Schaad relationship and the rule of the geometric mean). In addition, the studies that suggest coupled motion in ADH all looked at the oxidation of the alternative substrate benzyl alcohol to aldehyde, rather than at the oxidation of the natural substrate. Experiments performed with dihydrofolate reductase (DHFR) revealed no such breakdown of the RGM, and hence suggest the absence of any coupled motions. Thus, until other systems are studied in a similar fashion and also show signs of coupled motion,  $2^\circ$  SSEs must be interpreted with caution.

### 7.4.1 Alcohol Dehydrogenase

Alcohol dehydrogenases (ADHs) catalyse the reversible conversion of alcohols to aldehydes, using  $\text{NAD}^+$  as the oxidising agent. Yeast and horse liver alcohol dehydrogenases, and a thermophilic ADH from *Bacillus stearothermophilus* (YADH, HLADH, and *bsADH*, respectively) have been studied extensively in the context of tunnelling and coupled motion. For HLADH and selected mutants,  $2^\circ$  KIEs were measured using mixed-labelling experiments, and deviations from  $2^\circ$   $^{\text{M}}\text{SSE}$  were observed. These studies yielded two particularly interesting results:<sup>38–40</sup> (i) X-ray crystallography and KIE measurements suggested that  $2^\circ$   $^{\text{M}}\text{SSE}$  increases with decreasing distance between donor and acceptor<sup>40</sup> and (ii) for an entire set of mutants, the catalytic efficiency ( $k_{\text{cat}}/K_{\text{m}}$ ) and the  $2^\circ$   $^{\text{M}}\text{SSE}$ s appear correlated.<sup>39</sup> The first result suggests that the donor–acceptor distance (*i.e.* the tunnelling barrier width) indeed plays a critical role in the  $1^\circ$ – $2^\circ$  coupled motion and tunnelling, while the second result indicates the importance of  $1^\circ$ – $2^\circ$  coupled motion to the catalysed reaction.

For the thermophilic *bsADH*, small KIEs were reported ( $\sim 3$ ) along with large enthalpies of activation and the KIEs were temperature independent at the physiological temperature of this thermophile ( $75^\circ\text{C}$ ).<sup>41,42</sup> At temperatures much lower than the physiological temperature ( $30^\circ\text{C}$ ), however, the KIEs became

temperature dependent. These data can be interpreted using a Marcus-like model of tunnelling as having perfect prearrangement (no gating required) at physiological temperature but poor prearrangement (significant gating) at low temperature. In addition, measured  $2^\circ$  MSSEs were inflated (much larger than 3.3 and up to 15!) at the physiological temperature and sharply decreased at temperatures below  $30^\circ\text{C}$  toward semiclassical values. This decrease in  $2^\circ$  MSSEs was accompanied by an increase in the enthalpy of activation (14.6 to 23.6 kcal/mol for H-transfer; 15.1 to 31.4 kcal/mol for D-transfer). The mechanistic phase transition was accompanied by an increase in the rigidity of the protein.<sup>42–44</sup> Together, these results indicate a decrease in tunnelling contributions, or a change in the tunnelling properties, at lower temperatures. This finding can be interpreted by considering the increased rigidity of the enzyme at low temperatures.

## 7.4.2 Dihydrofolate Reductase

Dihydrofolate reductase (DHFR) is an essential participant in folic acid metabolism, catalysing the conversion of 7,8-dihydrofolate ( $\text{H}_2\text{F}$ ) to 5,6,7,8-tetrahydrofolate ( $\text{H}_4\text{F}$ ), with nicotinamide adenine dinucleotide phosphate (NADPH) acting as the hydride donor. The reaction involves transfer of the pro-R hydride from C4 of NADPH to C6 of  $\text{H}_2\text{F}$ , with concurrent reduction at the N5 of the  $\text{H}_2\text{F}$ . The small-size and well-characterised kinetic and mechanistic pathways of DHFR, and its biological importance, make it an attractive subject of studies in protein dynamics.<sup>45</sup> The complex kinetic pathway of DHFR has been extensively studied.<sup>46</sup>

Recently,  $1^\circ$  H/T and D/T KIEs were measured for DHFR across a temperature range of  $5\text{--}45^\circ\text{C}$  and the temperature dependence of the intrinsic KIEs was calculated.<sup>47</sup> The intrinsic KIEs were found to be temperature independent. The intrinsic  $1^\circ\text{H/D}$  KIE was  $3.5 \pm 0.2$ , a value that is nearly identical to the KIE of 3.4 calculated from mixed quantum/molecular-dynamics simulations.<sup>48</sup> The  $A_{\text{H}}/A_{\text{T}}$  was  $7.2 \pm 3.5$ , much above the semiclassically expected value. This kind of temperature dependence is indicative of perfect prearrangement of the tunnelling conformations (see Chapter 5). Three, distal mutants were also studied (G121V, M42W and G121V-M42W).<sup>49–51</sup> The mutants were found to exhibit different tunnelling patterns from the wild type (WT) and from each other: while the WT enzyme required no modification of the donor–acceptor distance to facilitate tunnelling, the single mutants did require some rearrangement to arrive at the appropriate tunnelling distance. The double mutant, on the other hand, required significant rearrangement before tunnelling could occur, thus showing a stronger temperature dependence than either of the single mutants.

The finding that mutations at remote residues affected the tunnelling behaviour at the active site suggest the presence of a network of residues that are remote from the active site but are dynamically coupled to the reaction chemistry. The results of these studies are supported by hybrid quantum/classical-molecular-dynamics simulations.<sup>52–54</sup>

### 7.4.3 Thymidylate Synthase

Thymidylate synthase catalyses the reductive methylation of 2'-deoxyuridine-5'-monophosphate (dUMP) to 2'-deoxythymidine-5'-monophosphate (dTMP).  $N^5,N^{10}$ -methylene-5,6,7,8-tetrahydrofolate acts as both a methylene and a hydride donor.<sup>55</sup> Recent studies on the hydride-transfer step using competitive H/T and D/T KIEs resulted in the calculation of temperature independent intrinsic KIEs, with H/T values close to 7 and  $A_H/A_T = 6.8 \pm 2.8$ . Interestingly, the reaction had a small enthalpy of activation ( $E_a = 4.0 \pm 0.1$  kcal/mol).<sup>48</sup> As for the DHFR findings presented above, the results with thymidylate synthase could not be explained simply by the tunnelling regimes defined in Section 7.3.4. Models that separated the temperature dependence of the isotopically sensitive and insensitive steps, namely Marcus-like models, rationalised the findings. Thus, the temperature-dependent rates are explained as arising from the isotopically insensitive preorganisation of the system, while the temperature-independent KIEs arise due to the isotopically sensitive tunnelling step.

## 7.5 Conclusions

The measurement of kinetic isotope effects can play a dramatic role in clarifying the mechanistic and kinetic details of complex enzymatic reactions. In the context of tunnelling, the size and temperature dependence of the KIEs, as well as the Swain–Schaad relationships, can indicate tunnelling in a system. The advantage of KIE measurements lies in their ability to follow changes in the transition state of the reaction, while causing minor disruptions (at most) of the reaction potential surface (isotopes do not affect the electronic configuration of the molecules). As demonstrated in Section 7.2, obstacles such as kinetic complexity can be overcome by using judicious labelling patterns in the KIE experiment, and intrinsic KIEs can be calculated that provide insight into the potential surface of the reaction. Furthermore, experimental measurements of the temperature dependence of KIE have contributed to the development of Marcus-like models of tunnelling. These models are better able to explain different cases of temperature dependence of KIEs, and can shed light on the role of tunnelling and enzyme dynamics in catalysis.

## Uncited References

19

## References

1. A. Fersht, *Structure and Mechanism in Protein Sciences: A Guide to Enzyme Catalysis and Protein Folding*, W. H. Freeman, New York, 1998.
2. W. P. Jencks, *Catalysis in Chemistry and Enzymology*, McGraw-Hill, New York, 1987.

3. L. Melander and W. H. Saunders, *Reaction Rates of Isotopic Molecules*, R.E. Krieger, Malabar, FL, 1987.
4. A. Kohen and J. P. Klinman, *Acc. Chem. Res.*, 1998, **31**, 397.
5. J. Bigeleisen and M. G. Mayer, *J. Chem. Phys.*, 1947, **15**, 261.
6. J. Bigeleisen and M. Wolfsberg, *Adv. Chem. Phys.*, 1958, **1**, 15.
7. P. M. Kiefer and J. T. Hynes, *J. Phys. Chem. A*, 2003, **107**, 9022.
8. W. P. Huskey and R. L. Schowen, *J. Am. Chem. Soc.*, 1983, **105**, 5704.
9. D. Ostovic, R. M. G. Roberts and M. M. Kreevoy, *J. Am. Chem. Soc.*, 1983, **105**, 7629.
10. A. Kohen and J. Jensen, *J. Am. Chem. Soc.*, 2002, **124**, 3858.
11. J. Rucker and J. P. Klinman, *J. Am. Chem. Soc.*, 1999, **121**, 1997.
12. J. Pu, S. Ma, M. Garcia-Viloca, J. Gao, D. J. Truhlar and A. Kohen, *J. Am. Chem. Soc.*, 2005, **127**, 14879.
13. C. G. Swain, E. C. Stivers, J. F. Reuwer and L. J. Schaad, *J. Am. Chem. Soc.*, 1958, **80**, 5885.
14. W. W. Cleland, in *Isotope Effects, in Chemistry and Biology*, ed. A. Kohen and H. H. Limbach, Taylor & Francis, CRC Press, Boca Raton, FL, 2006, p. 915.
15. D. B. Northrop, in *Isotope Effects in Chemistry and Biology*, ed. A. Kohen and H. H. Limbach, Taylor & Francis, CRC Press, Boca Raton, FL, 2006, p. 837.
16. W. E. Karsten and P. F. Cook, in *Isotope effects, in Chemistry and Biology*, ed. A. Kohen and H. H. Limbach, Taylor & Francis, CRC Press, Boca Raton, FL, 2006, p. 794.
17. D. B. Northrop, in *Isotope Effects on Enzyme-catalysed Reactions*, ed. W. W. Cleland, M. H. O'Leary and D. B. Northrop, University Park Press, Baltimore, MD, 1977, p. 122.
18. D. B. Northrop, in *Enzyme Mechanism from Isotope Effects*, ed. P. F. Cook, CRC Press, Boca Raton, FL, 1991, p. 181.
19. W. W. Cleland, *Adv. Enzymol.*, 1977, **45**, 273.
20. D. W. Parkin, in *Enzyme Mechanism from Isotope Effects*, ed. P. F. Cook, CRC Press, Boca Raton, FL, 1991, p. 269.
21. W. H. Saunders, *J. Am. Chem. Soc.*, 1985, **107**, 164.
22. A. Kohen, in *Isotope Effects in Chemistry and Biology*, ed. A. Kohen and H. H. Limbach, Taylor & Francis CRC Press, Boca Raton, FL, 2006, p. 743.
23. W. P. Huskey, *J. Phys. Org. Chem.*, 1991, **4**, 361.
24. W. H. Saunders, *Croat. Chem. Acta*, 1992, **65**, 505.
25. S. Lin and W. H. Saunders, *J. Am. Chem. Soc.*, 1994, **116**, 6107.
26. J. Hirschi and D. A. Singleton, *J. Am. Chem. Soc.*, 2005, **127**, 3294.
27. T. Jonsson, M. H. Glickman, S. J. Sun and J. P. Klinman, *J. Am. Chem. Soc.*, 1996, **118**, 10319.
28. M. M. Whittaker, D. P. Ballou and J. W. Whittaker, *Biochemistry*, 1998, **37**, 8426.
29. M. H. Glickman and J. P. Klinman, *Biochemistry*, 1995, **34**, 14077.
30. W. W. Cleland and J. S. Blanchard, *Biochemistry*, 1980, **19**, 3543.

31. J. D. Hermes, S. W. Morrical, M. H. O'Leary and W. W. Cleland, *Biochemistry*, 1984, **23**, 5479.
32. Z. Smedarchina and W. Siebrand, *Chem. Phys. Lett.*, 2005, **410**, 370.
33. C. S. Tautermann, M. J. Loferer, A. F. Voegelé and K. R. Liedla, *J. Chem. Phys.*, 2004, **120**, 11650.
34. J. Bigeleisen, *J. Chem. Phys.*, 1955, **23**, 2264.
35. J. P. Klinman, *Philos. Trans. Royal Soc. B*, 2006, **361**, 1323.
36. D. G. Truhlar and A. Kohen, *Proc. Natl. Acad. Sci. USA*, 2001, **98**, 848.
37. A. Kohen and J. P. Klinman, *Chem. Biol.*, 1999, **6**, 191.
38. B. J. Bahnson, D. H. Park, K. Kim, B. V. Plapp and J. P. Klinman, *Biochemistry*, 1993, **32**, 5503.
39. B. J. Bahnson, T. D. Colby, J. K. Chin, B. M. Goldstein and J. P. Klinman, *Proc. Natl. Acad. Sci. USA*, 1997, **94**, 12797.
40. T. D. Colby, B. J. Bahnson, J. K. Chin, J. P. Klinman and B. M. Goldstein, *Biochemistry*, 1998, **37**, 9295.
41. A. Kohen, R. Cannio, S. Bartolucci and J. P. Klinman, *Nature*, 1999, **399**, 496.
42. A. Kohen and J. P. Klinman, *J. Am. Chem. Soc.*, 2000, **122**, 10738.
43. C. E. Atreya, E. F. Johnson, J. Williamson, S. Y. Chang, P. H. Liang and K. S. Anderson, *J. Biol. Chem.*, 2003, **278**, 28901.
44. Z. X. Liang, T. Lee, K. A. Resing, N. G. Ahn and J. P. Klinman, *Proc. Natl. Acad. Sci. USA*, 2004, **101**, 9556.
45. S. Hammes-Schiffer and S. J. Benkovic, *Annu. Rev. Biochem.*, 2006, **75**, 519.
46. C. A. Fierke, K. A. Johnson and S. J. Benkovic, *Biochemistry*, 1987, **26**, 4085.
47. R. S. Sikorski, L. Wang, K. A. Markham, P. T. R. Rajagopalan, S. J. Benkovic and A. Kohen, *J. Am. Chem. Soc.*, 2004, **126**, 4778.
48. N. Agrawal, B. Hong, C. Mihai and A. Kohen, *Biochemistry*, 2004, **43**, 1998.
49. L. Wang, S. Tharp, T. Selzer, S. J. Benkovic and A. Kohen, *Biochemistry*, 2006, **45**, 1383.
50. L. Wang, N. M. Goodey, S. J. Benkovic and A. Kohen, *Philos. Trans. Royal Soc. B*, 2006, **361**, 1307.
51. L. Wang, N. M. Goodey, S. J. Benkovic and A. Kohen, *Proc. Natl. Acad. Sci. USA*, 2006, **103**, 15753.
52. P. K. Agarwal, S. R. Billeter, P. T. R. Rajagopalan, S. J. Benkovic and S. Hammes-Schiffer, *Proc. Natl. Acad. Sci. USA*, 2002, **99**, 2794.
53. J. B. Watney, P. K. Agarwal and S. Hammes-Schiffer, *J. Am. Chem. Soc.*, 2003, **125**, 3745.
54. A. Warshel and H. Liu, *J. Phys. Chem. B*, 2007, **111**, 7852.
55. D. V. Santi and C. F. Brewer, *J. Am. Chem. Soc.*, 1968, **90**, 6236.